Covalent Attachment of Cell-Adhesive, (Arg-Gly-Asp)-Containing Peptides to Titanium Surfaces

ARTICLE *in* LANGMUIR · SEPTEMBER 1998

Impact Factor: 4.46 · DOI: 10.1021/la980257z

Covalent Attachment of Cell-Adhesive, (Arg-Gly-Asp)-Containing Peptides to Titanium Surfaces

Shou-Jun Xiao, Marcus Textor, and Nicholas D. Spencer*

Laboratory for Surface Science and Technology, Department of Materials, Swiss Federal Institute of Technology, ETH-Zürich, CH-8092 Zürich, Switzerland

Hans Sigrist

CSEM (Centre Suisse d'Electronique et de Microtechnique SA), Jaquet-Droz 1, CH-2007 Neuchâtel, Switzerland

Received March 3, 1998. In Final Form: June 18, 1998

A three-step reaction procedure was applied to introduce RGD-containing peptides on the titanium surface. Water−vapor−plasma-pretreated titanium surfaces were first silanized with (3-aminopropyl)-triethoxysilane, resulting in a multilayer film of poly(3-aminopropyl)siloxane. In a second reaction step, the free primary amino groups were linked to one of the three hetero-cross-linkers: *N*-succinimidyl-6-maleimidylhexanoate, *N*-succinimidyl-3-maleimidylpropionate, and *N*-succinimidyl *trans*-4-(maleimidyl-methyl)cyclohexane-1-carboxylate. Onto the resulting terminal-maleimide surface, two model, cell-adhesive peptides, H-Gly-Arg-Gly-Asp-Ser-Pro-Cys-OH and H-Arg-Gly-Asp-Cys-OH were immobilized through covalent addition of the cysteine thiol (−SH) group. X-ray photoelectron spectroscopy, infrared reflection absorption spectroscopy, and radiolabeling techniques were applied to characterize the surfaces. From independent quantitative analysis, an approximate coverage of 0.2∼0.4 peptides/nm^2 was calculated.

1. Introduction

Much attention has recently been directed toward the development of bioactive and biocompatible material surfaces for a variety of technological applications, among them biosensors,[1] bioreactors,[2] chromatographic supports,[3] and functionalized building blocks for biomaterials.[4] A major challenge in the development of functional surfaces is to devise strategies, employing either existing synthetic technologies or novel fabrication methods, to assemble various complex molecular species on material surfaces, such as organized thin organic films functionalized with peptides, proteins, or DNA/RNA strands. To select appropriate synthetic routes, the following restrictions have to be considered: (1) The attachment site and chemistry must not interfere with the functional structure or the active site of the biomolecule, (2) the attached biomolecule must not be denatured or inactivated at the surface during or following attachment, and (3) the attached biomolecule should be stably bound at the surface through linkages that are not susceptible to disruption by hydrolysis or other interactions with species in the environment.

Titanium is a successful biocompatible material that is extensively used today for manufacturing bone-anchoring systems, such as dental implants or hip-joint fixation and replacement, as well as for pacemakers, heart valves, and ear-drum drainage tubes. It has advantageous bulk and surface properties: in particular, a low modulus of elasticity, a high strength-to-weight ratio, excellent resistance to corrosion, and an inert, biocompatible surface oxide film.[5] The surface chemistry and structure are prime factors governing bone integration[6] and there is—from the standpoint of both surgeon and patient—considerable interest in increasing both speed of formation (healing time) and degree (long-term success) of close bone aposition for cement-free implantation. To further improve the biocompatibility of titanium, many physical and chemical surface modification methods such as electrochemical oxidation, plasma coating with titanium or hydroxyapatite, and ion implantation are in use.[7] Reports concerning biochemical modification to change a bioinert surface to a bioactive surface, however, are rare. One example is a paper by Sukenik et al.[8] describing the modification of the titanium surface with terminal groups such as CH_3, OH, and Br through silanization and their biological effect in neural cell culture tests.

The amino acid sequence RGD (Arg-Gly-Asp) is present in many extracellular matrix (ECM) proteins and has been found to play an important role in cellular growth, differentiation, proliferation, and regulation of overall cell function.[9] Immobilized, synthetic, RGD-containing peptides on solid supports such as polymers[10] and silicon oxide surfaces[11] have been reported to mediate specific surface−cell interactions and to promote cell organization. Studies of cell migration suggest the importance of the surface density of RGD sequences for efficient cell−matrix interaction.[12]

* To whom correspondence should be addressed.

(1) Schultz, J. S. *Sci. Am.* **1991**, *265*, 64.
(2) Fodor, S. P. A.; Read, L.; Pirrung, M. C.; Stryer, L.; Lu, A. T.; Solas, D. *Science* **1991**, *251*, 767.
(3) Nawrocki, J.; Dunlap, J.; Carr, P. W.; Blackwell, J. A. *Biotechnol. Prog.* **1994**, *10*, 561.
(4) Ratner, B. D. *J. Mol. Rec.* **1996**, *9*, 617.
(5) Brown, S. A.; Lemons, J. E. *Medical Application of Titanium and Its Alloys: The Material and Biological Issues;* ASTM: Philadelphia, PA, 1996.
(6) Doherty, P. J.; Williams, D. F. *Biomaterial-Tissue Interfaces: Advances in Biomaterials;* Elsevier: New York, 1992; Vol. 10.
(7) Geckeler, K. E.; Rupp, F.; Geis-Gerstorfer, J. *J. Adv. Mater.* **1997**, *9*, 513 and references therein.
(8) Sukenik, C. N.; Balachander, N.; Culp, L. A.; Lewandowska, K.; Merritt, K. *J. Biomed. Mater. Res.* **1990**, *24*, 1307.
(9) Ruoslahti, E.; Pierschbacher, M. D. *Science* **1987**, *238*, 491.
(10) Glass, J. R.; Dickerson, K. T.; Stecker, K.; Polarek, J. W. *Biomaterials* **1996**, *17*, 1101.
(11) Massia, S. P.; Hubbell, J. A. *Anal. Biochem.* **1990**, *187*, 292.
(12) Brandly, B. K.; Schaar, R. L. *Anal. Biochem.* **1988**, *172*, 270.

S0743-7463(98)00257-1 CCC: $15.00
Published on Web 08/21/1998

The most commonly used immobilization methods on inorganic oxide surfaces involve reactively deposited silane films with terminal functional groups that can be further modified with different linking moieties. For aminosilanes, a variety of routes for further modification have been applied, for example, (1) reaction with glutaraldehyde,[13] yielding an aldehyde that can form an imine linkage with primary amines on the peptides, or (2) reaction with a mixture of peptides and carbodiimides, yielding an amide linkage with carboxyl groups on the peptides.[14] The two methods utilize the primary amino groups and carboxyl groups that occur with high frequency in peptides and proteins, but specific attachment at a defined site is very difficult with these functionalities. It is apparent that these approaches must produce highly heterogeneous surfaces.

The most recently examined method employs heterobifunctional cross-linkers with both thiol- and amino-reactive moieties,[15,17−21] which have been widely used in protein conjugation and cross-linking.[16] Bathia et al.[17] linked the maleimidyl group onto thiol-terminal silanized silica surfaces, followed by immobilization of *anti*-IgG antibody through the reaction of the primary amine moieties with the succinimidyl ester. Hong et al.[18] achieved the attachment of cytochrome by reaction of a succinimidyl ester with amine-terminated, silanized glass surfaces, followed by covalent binding of a single unique cysteine thiol on the cytochrome through maleimide. Using similar chemistry, Heyse et al.[19] attached thiol-bearing phospholipids onto optical waveguide surfaces (SiO_2-TiO_2 waveguide layer); Chrisey et al.[20] immobilized DNA on silica surfaces; Matsuzawa et al.[21] attached a synthetic peptide on glass for neuron culture tests. This functionalization technique satisfies to some extent the aforementioned requirements: production of a single functional site and mild reaction conditions. A particular advantage is the much higher surface coverage of biomolecules with this method compared to other coupling approaches. Although the surfaces were characterized by radiolabeling and UV−vis spectroscopy and subjected to biological activity assays, our knowledge regarding the physicochemical properties of these surfaces is still rudimentary.

In a recent publication,[22] we described the binding of H-Arg-Gly-Asp-Cys-OH (RGDC) onto a maleimide-functionalized surface. The present paper extends the studies to the binding of H-Gly-Arg-Gly-Asp-Ser-Pro-Cys-OH (GRGDSPC) as well as the use of a variety of surface functionalization and characterization techniques. The aim of the work is to covalently bind cell-adhesive RGD-containing peptides onto Ti surfaces and to evaluate the biocompatibility of these novel surfaces. Both surface-specific techniques (X-ray photoelectron spectroscopy (XPS), infrared reflection absorption spectroscopy (IRAS), ellipsometry, and contact angle goniometer) and radiolabeling methods were used to qualitatively and quantitatively characterize the surfaces after each reaction step. Good agreement is achieved between XPS and radiolabeling techniques in regard to the quantitative estimation of surface coverages. The results of cell culture tests and the biocompatibility performance of these novel surfaces will be published separately.

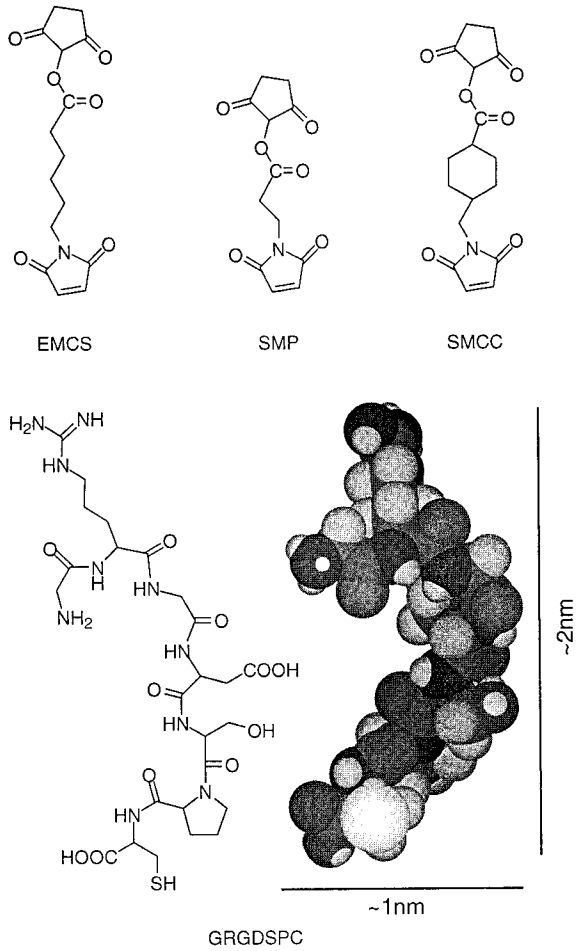

Figure 1. Molecular structures of the three cross-linkers: EMCS, SMP, SMCC, and the peptide GRGDSPC. The space-filling model of GRGDSPC with the minimum energy conformation calculated from MM2 is also shown.

2. Materials and Methods

2.1. Materials. The 100-nm-thick Ti coatings were produced on both sides of round glass cover slips (diameter = 15 mm, thickness = 0.16 mm) (Huber & Co. AG, Reinach/Switzerland) in a Leybold Z600 DC-magnetron sputtering facility.[23] Under the same conditions, larger Ti substrates (2×5 cm^2) were also prepared for IRAS measurements. For the plasma treatment, a plasma cleaner/sterilizer PDC-32G (Harrick, New York) was used. Pure water was obtained from an EASYpure device, Barnstead, USA. (3-Aminopropyl)triethoxysilane (APTES) was bought from Fluka, Buchs, Switzerland, distilled, stored, and used under N_2. The hetero-cross-linkers, *N*-succinimidyl-6-maleimidylhexanoate (EMCS), *N*-succinimidyl-3-maleimidylpropionate (SMP) (Fluka), *N*-succinimidyl *trans*-4-(maleimidylmethyl)cyclohexane-1-carboxylate (SMCC) (Molecular Probe,

(13) Puleo, D. A. *Biomaterials* **1996**, *17*, 217.
(14) (a) Dee, K. C.; Andersen, T. T.; Bizios, R. *Tissue Eng.* **1995**, *1*, 135. (b) Dee, K. C.; Rueger, D. C.; Andersen, T. T.; Bizios, R. *Biomaterials* **1996**, *17*, 209.
(15) Jonsson, U.; Malmqvist, M.; Olofsson, G.; Ronnberg, I. In *Methods in Enzymology*; Mosbach, K., Ed.; Academic Press: San Diego, 1988; Vol. 137, p 381.
(16) Wong, S. S. *Chemistry of Protein Conjugation and Cross-linking*; CRC Press: Boca Raton, FL, 1991.
(17) Bhatia, S. K.; Shriver-Lake, L. C.; Prior, K. J.; Georger, J. H.; Calvert, J. M.; Bredehorst, R.; Ligler, F. S. *Anal. Biochem.* **1989**, *178*, 408.
(18) (a) Hong, H.-G.; Bohn, P. W.; Sligar, S. G. *Anal. Chem.* **1993**, *65*, 1635. (b) Hong, H.-G.; Jiang, M.; Sliger, S. G.; Bohn, P. W. *Langmuir* **1994**, *10*, 153.
(19) Heyse, S.; Vogel, H.; Sanger, M.; Sigrist, H. *Protein Chem.* **1995**, *4*, 2532.
(20) (a) Chrisey, L. A.; Lee, G. U.; O'Ferrall, C. E. *Nucleic Acids Res.* **1996**, *24*, 3031. (b) Lee, G. U.; Chrisey, L. A.; O'Ferrall, C. E.; Pilloff, D. E.; Turner, N. H.; Colton, R. J. *Israel J. Chem.* **1996**, *36*, 81.
(21) Matsuzawa, M.; Umemura, K.; Beyer, D.; Sugioka, K.; Knoll, W. *Thin Solid Films* **1997**, *305*, 74.
(22) Xiao, S. J.; Textor, M.; Spencer, N. D.; Wieland, M.; Keller, B.; Sigrist, H. *J. Mater. Sci. Mater. Med.* **1997**, *8*, 867.
(23) Kurrat, R.; Textor, M.; Ramsden, J. J.; Böni, P.; Spencer, N. D. *Rev. Sci. Instrumen.* **1997**, *68*, 2172.

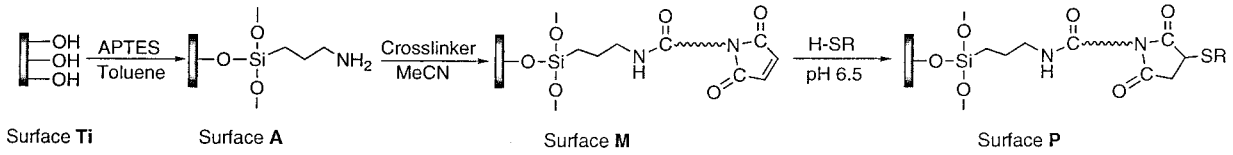

Figure 2. Schematic representation of the modification route. Surface **Ti**: water−vapor−plasma-pretreated titanium. Surface **A**: poly(3-aminopropyl)siloxane pendant surface. Surface **M**: maleimide-modified surfaces with different alkyl chains. Surface **P**: peptide- or L-cysteine-modified surfaces. H−SR: L-cysteine, RGDC, and GRGDSPC.

Netherlands), were stored as recommended by the supplier. The radiolabeling reagents, [^{14}C]-formaldehyde ([^{14}C]-FA) with specific radioactivity 54.0 mCi/mmol, [^{35}S]-L-cysteine ([^{35}S]-Cys) with 20−150 mCi/mmol, and [^{14}C]-phenylglyoxal ([^{14}C]-PG) with 27.0 mCi/mmol, were purchased from Amersham, Buckinghamshire, U.K., stored, and used as indicated. RGDC (65.2%) and GRGDSPC (65%) were purchased from Bachem AG, Bubendorf, Switzerland, and all other chemicals were obtained from Fluka.

The molecular structures of cross-linkers and GRGDSPC are illustrated in Figure 1.

2.2. Surface Modification Route. The surface modification route is shown in Figure 2. Water−vapor−plasma-pretreated titanium surfaces were first activated by APTES, followed by reaction of terminal amines with succinimidyl esters of the cross-linkers, and finally by the covalent binding of the thiol-bearing RGD-containing peptides through maleimidyl groups.

The different surfaces are defined as follows: **Ti**, water−vapor−plasma-pretreated titanium surface; **A**, poly(3-aminopropyl)siloxane-modified surface; **^{14}CA**, [^{14}C]-formaldehyde + **A**; **M**, maleimide-modified surface; **MH**, *N*-maleimidyl-6-hexanoyl (MH) pendant surface; **^{35}SMH**, [^{35}S]-L-cysteine + **MH**; **MP**, *N*-maleimidyl-3-propanoyl (MP) pendant surface; **MC**, *trans*-4-(maleimidylmethyl)cyclohexane-1-carbonyl (MC) pendant surface; **P**, peptide- or l-cysteine-modified surface; **CMH**, L-cysteine + **MH**; **CMP**, L-cysteine + **MP**; **CMC**, L-cysteine + **MC**; **GMH**, GRGDSPC + **MH**; **RMH**, RGDC + **MH**; **GMP**, GRGDSPC + **MP**; **RMP**, RGDC + **MP**; **GMC**, GRGRSPC + **MC**; **RMC**, RGDC + **MC**; **^{14}CGMH**, [^{14}C]-phenylglyoxal + **GMH**.

2.3. Chemical Functionalization. Preparation of Silanized Samples. Prior to silanization, the titanium-coated glass cover slips were first pretreated by water−vapor−plasma cleaning (0.42 mbar, 2 min) and then dried in a vacuum for 1 h. Three hundred samples of **Ti** were incubated using a self-fabricated glass holder in 200 mL of dry toluene containing 2 mL of APTES (43 mM) at 80 °C for 48 h. After reaction, the substrates were ultrasonically washed with chloroform five times, acetone twice, and methanol five times, and were extensively rinsed with water, then dried in a vacuum, and cured at 100 °C under N_2 for 1 h. The treated samples (**A**) were stored under argon for further reactions as detailed below.

Five samples of type **A** were acetylated by overnight treatment at room temperature with a mixture of toluene (1 mL), acetic acid anhydride (100 μL), and dry pyridine (100 μL). After 12 h, the samples were rinsed with toluene, CH_2Cl_2, and ethanol.

Preparation of Maleimide- (M) and Peptide- (or L-Cysteine-) Modified (P) Samples. Twenty silanized titanium samples (**A**) were placed in a self-fabricated polypropylene vessel with 2 mL of acetonitrile (CH_3CN) containing 5.0 mM cross-linkers. After incubation at 20 °C for 30 min, with 30 s of sonication every 10 min, the excess cross-linker solution was removed and the samples were washed extensively with acetonitrile, acetone, and hexane. After they were dried with N_2, the samples were subject to the next chemical step. Twenty maleimide-grafted substrates were incubated at 20 °C for 1 h in 2 mL of water containing 2.0 mM peptide or L-cysteine, with 30 s of sonication every 10 min. The pH of the peptide or l-cysteine solution was adjusted to 6.5 with 0.1 M NaOH before injection. The peptide-grafted substrates were washed thoroughly with water, dried with N_2, and stored in argon.

2.4. Surface Analysis Methods. X-ray Photoelectron Spectroscopy (XPS) Measurements. XPS spectra were recorded using a Specs SAGE 100 system with unmonochromatized Mg Kα radiation at 300 W (12 kV). Measurements were carried out using a takeoff angle of 90° with respect to the sample surface. The analyzed area was typically 9 × 9 mm^2. Survey scans over a binding energy range of 0−1150 eV were taken for each sample with a constant detector pass energy range of 50 eV, followed by a high-resolution XPS measurement (pass energy 14 eV) for quantitative determination of binding energy and atomic concentration. Background subtraction, peak integration, and fitting were carried out using SpecsLab software. Electron binding energies were calibrated to the hydrocarbon C 1s at 284.6 eV on pure titanium surfaces. To convert peak areas to surface concentration, sensitivity factors published by Evans et al. were used.[24]

Infrared Reflection Absorption Spectroscopy (IRAS) Measurements. The IRAS measurements were performed on a Bruker IFS 66V spectrometer operating at approximately 100 Pa. A mercury−cadmium−telluride (MCT) detector was used to collect spectra with a resolution of 2 cm^{-1}. The angle of incidence was 80° from the surface normal. A water−vapor−plasma-pretreated Ti mirror was used as the reference. For both sample and reference, 500 scans were collected.

Ellipsometry Measurements. Film thickness was measured by means of a Gaertner L-116C ellipsometer and software. The angle of incidence was set at 70°. The optical constants of surface **Ti** were determined in at least four different areas on each individual substrate. The thickness of the modified organic films was calculated using the software for a single organic thin film and a refractive index of 1.40. They are about 2-, 3-, and 4-nm thick for surface **A**, **MH**, and **GMH**, respectively.

Contact Angle Measurements. Advancing contact angles were measured on a Ramé-Hart NRL model goniometer at room temperature and ambient humidity. For the measurements, 6 μL of water was put on the surface, followed by adding another 6 μL to the first drop. The contact angle was measured immediately within 1 min. They are 30°, 44°, 60°, and 45° for surfaces **Ti**, **A**, **MH**, and **GMH**, respectively. The experimental error of this method is estimated to be ±3°.

Radiolabeling Procedure. [^{14}C]-Formaldehyde labeling of surface **A** was performed in a self-fabricated metal sample holder with four wells (diameter = 7 mm). Acetonitrile (50 μL) containing 10.0 mM $NaBH_3CN$ and 2.0 mM [^{14}C]-formaldehyde was injected into each well. After incubation for 4 h at 20 °C, the excess radioactive solution was removed and the exposed surface washed with CH_3CN 10 times and water 10 times. The demounted samples were extensively washed again with water and then dried with N_2. The same procedure was also applied to the control surfaces of **Ti** and acetylated **A**. The radioactivity of each sample was measured by scintillation counting in 5 mL of scintillation fluid (1080 mL of toluene, 920 mL of Triton X-100, 5.4 g of 2,5-diphenyloxazole, 0.2 g of 1,4-bis-2-(5-phenyloxazolyl) benzene, and 40 mL of acetic acid) on a Tri-Carb 2300TR liquid scintillation counter (Packard Instrument Co., USA).

Maleimide-functionalized substrates (**M**), kept between two metal plates, were covered with 50 μL of 0.11 μCi/μL [^{35}S]-cysteine aqueous solution in each well. The pH of the solution was adjusted to 6.5 by 0.1 mM NaOH before use. After incubation for 1 h at 20 °C, the excess radioactive solution was rinsed off 10 times with water. The substrates were then removed from the metal plates, washed again with excess water, and dried with N_2, and the radioactivity was determined. Control experiments for the covalent binding of cysteine to maleimide-functionalized substrates were carried out as above by applying the same [^{35}S]-cysteine solution to surface **A** and unlabeled-L-cysteine-reacted surface **M**.

Radiolabeling of RGD-grafted surfaces was carried out by injecting 50 μL of sodium phosphate (25 mM) buffer (pH 7.4) containing 5 mM [^{14}C]-PG to each well as described above,

(24) Evans, S.; Pritchard, R. G.; Thomas, J. M. *J. Electron Spectrosc. Relat. Phenom.* **1978**, *14*, 341.

Table 1. XPS Binding Energies C 1s, N 1s, Ti 2p, and O 1s for the Surfaces Ti, A, MH, and GMH and the Proposed Assignments to Surface Functionalities

surface	C 1s region BE (eV), %, assignments	N 1s region BE (eV), %, assignments	Ti 2p region[b] BE (eV), %, assignments	O 1s region BE (eV), %, assignments
Ti	284.6 (100) hydrocarbon[a]		453.3 (5) $2p_{3/2}$ Ti metal 458.5 (63) $2p_{3/2}$ TiO_2 464.3 (32) $2p_{1/2}$ TiO_2	530.0 (84) TiO_2 531.7 (16) OH
A	285.0 (72) C−C 286.4 (22) C−N 288.3 (6) C═O[a]	399.6 (75) NH_2 401.7 (25) NH_3^+	453.3 (1) $2p_{3/2}$ Ti metal 458.5 (66) $2p_{3/2}$ TiO_2 464.3 (33) $2p_{1/2}$ TiO_2	530.0 (58) TiO_2 532.3 (42) SiO
MH	285.1 (56) C−C 286.3 (26) C−N 288.2 (6) amide-*C* 289 (12) imide-*C*	399.6 (21) NH_2 400.1 (25) amide-*N* 400.7 (30) imide-*N* 401.7 (24) NH_3^+	458.5 (67) $2p_{3/2}$ TiO_2 464.3 (33) $2p_{1/2}$ TiO_2	530.0 (48) TiO_2 532 3 (52) SiO, C═O
GMH	285.1 (51) C−C 286.3 (29) C−N,C−O 288.2 (9) amide-*C* 289.0 (11) imide-, carboxyl-, guanidinyl-*C*	399.6 (14) NH_2 400.1 (39) amide-*N* 400.7 (26) imide-*N* 401.7 (21) NH_3^+, guanidinyl-*N*	458.5 (67) $2p_{3/2}$ TiO_2 464.3 (33) $2p_{1/2}$ TiO_2	530.0 (45) TiO_2 532.3 (55) SiO, C═O, COOH, C−OH

[a] Trace contaminations. [b] The detailed deconvolution of Ti 2p to different titanium oxidation states; see ref 29.

incubating for 24 h at 20 °C, then washing thoroughly with water, drying with N_2, and counting as detailed above.

The degradation experiments were carried out with the radiolabeled surfaces, **^{14}CA**, **^{35}SMH**, and **^{14}CGMH** by measuring their specific radioactivity loss as a function of storage time in 5 mL of water at room temperature.

3. Results and Discussion

3.1. Silanization Procedure. Silanization is the crucial step in regard to subsequent reproducibility of the chemical functionalization. Although silanization has been extensively studied, the resulting structure, coverage, orientation, and organization of the layers have not yet been satisfactorily determined and are still the subject of controversy.[25] It is generally accepted that silanization on inorganic surfaces occurs by reaction of silanol groups with hydroxyl groups present on oxide surfaces. Due to the ability of the silane to polymerize at the surface, the siloxane film can be produced as a monolayer or multilayer, depending on substrates, silane properties, and reaction conditions. In general, long-alkyl-chain silanes tend to form monolayers, while short bifunctional silanes, such as aminosilanes, tend to form multilayers.

Pretreatment of the titanium surface is an essential prerequisite for reproducible silanization. Untreated titanium films (as sputtered) gave unsatisfactory results. Optimum surface cleanliness and reactivity were achieved through water−vapor−plasma treatment, although other pretreatments such as H_2O_2 or HCl also gave satisfactory results.

APTES was chosen to silanize the titanium surface. From our experience, the reaction media (aqueous or organic), temperature, concentration, ratio of reactants, incubation time, washing steps, and soforth influence the amount of APS on titanium surfaces, to different degrees. Silanization in aqueous media resulted in a low surface concentration of amines (atomic ratio N/Si < 0.5 from XPS), which was not beneficial for further modification. However, silanization in toluene produced an APS film with a consistently high concentration of amines (N/Si = 0.7, see section 3.2). Thin and smooth APS films can be produced by extended silanization (toluene, 80 °C, and 48 h), followed by a three-step washing procedure: apolar organic solvent, polar organic solvent, and water. Immersion in water is a very efficient way to obtain thin, smooth films.[26] To exclude batch-to-batch variations and get reproducible data for further modification, a large number of samples (300 pieces) were produced in one batch with the same reaction conditions, washing steps, and curing. Curing has been widely used to stabilize the siloxane films because it drives the surface derivatization reaction further to completion. As a result, the cured films are more resistant to hydrolysis. However, a long time (12 h) curing at 100 °C in air resulted in a pronounced reduction of the surface amine concentration, as a result of oxidation of primary amines to imines and nitriles.[27] This significantly reduced the reaction yield of the subsequent reaction step with succinimidyl ester. Curing for 1 h at 100 °C under N_2 gas was employed in the present study.

The surface coverage of amino groups on samples of this batch was determined as 6.0 NH_2 groups/nm^2 via reaction of the amine with [^{14}C]-formaldehyde. The surface coverage of hydroxyl groups on the TiO_2 surface was estimated to be 6 OH groups/nm^2.[28] One aminosilane molecule reacts with 2 or 3 OH groups on the TiO_2 surface. Considering the N/Si ratio of 0.7 (Table 2), 9 silicon atoms/nm^2 would be present for every 4−6 APS layers on surface **A**. However, this does not mean that there are less than 25% primary amines exposed to the surface, since the surface roughness enhances the total proportion of exposed amines.

3.2. Monitoring Reaction Steps by XPS. XPS was used to monitor each reaction step as it can provide information on chemical structure, atomic concentration, and surface contamination. Figure 3 shows the evolution of the XPS signals of C 1s, N 1s, Ti 2p, and O 1s from **Ti** to **A**, **MH**, and **GMH**. Table 1 lists the experimental XPS binding energies of the deconvoluted detailed spectra and the proposed assignments to chemical bonds/oxidation states based on chemical shifts. Figure 4 illustrates the changes of the atomic concentrations on the above surfaces. Surfaces modified with other cross-linkers and peptides gave results consistent with the proposed interpretation and are not presented here.

Water−Vapor−Plasma-Pretreated Titanium Surface (Ti). Spectra of surface **Ti** show three elements: Ti, O, and C. Ti $2p_{3/2}$ at 458.5 eV and Ti $2p_{1/2}$ at 464.3 eV are assigned to TiO_2; Ti $2p_{3/2}$ at 453.3 eV is due to Ti metal because the XPS information depth is greater than the

(25) Ulman, A. *Chem. Rev.* **1996**, *96*, 1533.
(26) Haller, I. *J. Am. Chem. Soc.* **1978**, *100*, 8050.
(27) Ondrus, D. J.; Boerio, F. J. *J. Colloid Interface Sci.* **1988**, *124*, 349.
(28) Yates, D. E.; James, R. O.; Healy, T. W. *J. Chem. Soc., Faraday Trans.* **1980**, *76*, 1.

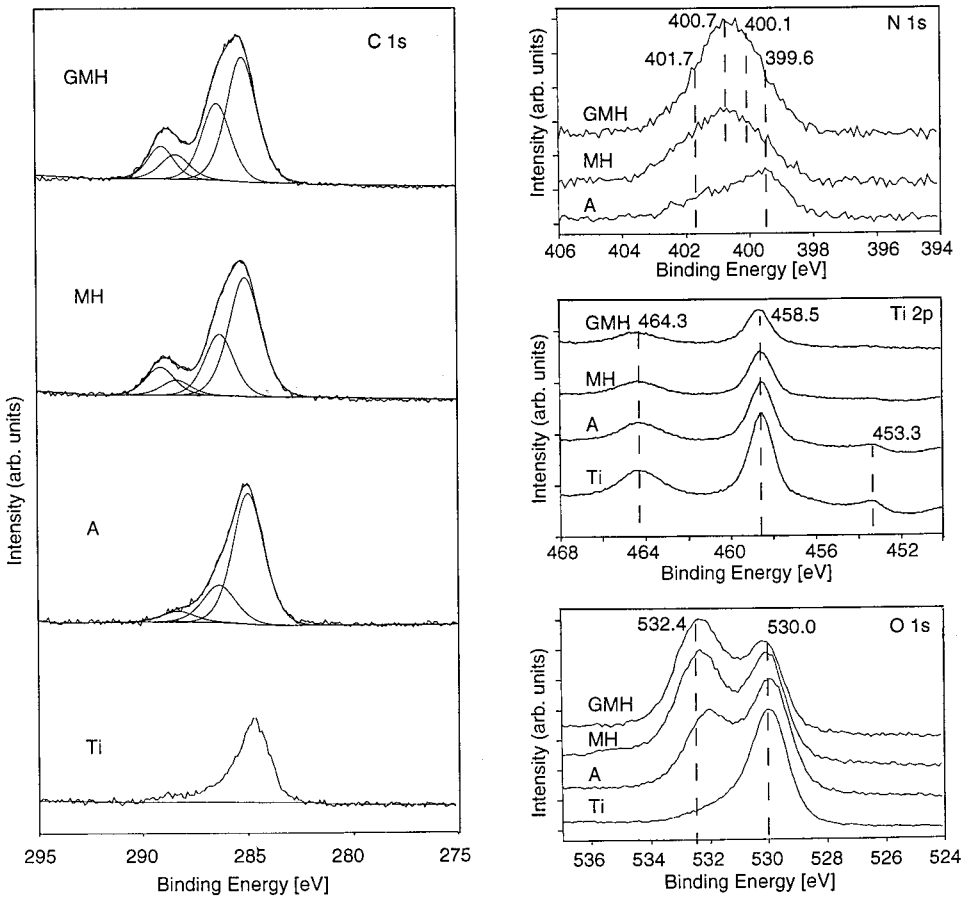

Figure 3. Results of the XPS surface analysis: evolution of C 1s, N 1s, Ti 2p, and O 1s spectra from **Ti** to **A**, **MH**, and **GMH**.

Table 2. XPS Atomic Ratios N/Si for APS-, Maleimide-, and Peptide- (or L-Cysteine-) Modified Surfaces and the Reaction Yields ($R_{X\rightarrow Y}$) Estimated Using Formulas 1 and 2 (See Text, Section 3.3)

surface	N/Si (±s.d.)	reaction ($X\rightarrow Y$)	$R_{X\rightarrow Y}$ % (± calculated error)
MH	0.95 ± 0.02	A → MH	36 ± 5
MP	0.90 ± 0.02	A → MP	29 ± 5
MC	0.87 ± 0.02	A → MC	24 ± 5
CMH	1.15 ± 0.04	MH → CMH	80 ± 20
CMP	1.05 ± 0.04	MP → CMP	75 ± 25
CMC	1.00 ± 0.04	MC → CMC	76 ± 32
RMH	1.26 ± 0.03	MH → RMH	15 ± 3
RMP	1.15 ± 0.04	MP → RMP	18 ± 4
RMC	1.05 ± 0.03	MC → RMC	15 ± 4
GMH	1.40 ± 0.04	MH → GMH	18 ± 3
GMP	1.26 ± 0.03	MP → GMP	18 ± 3
GMC	1.20 ± 0.03	MC → GMC	19 ± 4

thickness of the native TiO_2 layer (~5 nm).[29] O 1s at 530.0 eV is typical for TiO_2, while C 1s at 284.6 eV is due to the environmental hydrocarbon contamination.

Silanized Surface (A). XPS has shown[22] to be a powerful tool for following the silanization reaction from surface **Ti** to **A** via the appearance of N (N 1s at around 400 eV) and Si (Si 2p at 102.0 and 153.0 eV), as well as the new high binding energy peak of O 1s at 532.3 eV due to Si−O. The broad N 1s peak can be deconvoluted into two peaks 399.6 eV (75%) due to free amines and 401.7 eV (25%) assigned to protonated amines.[30]

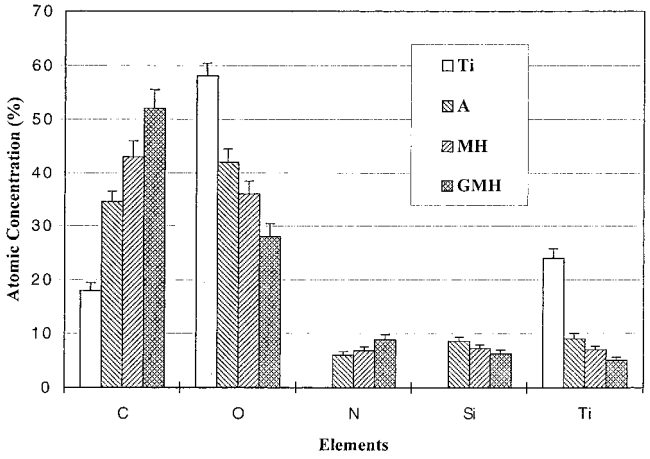

Figure 4. Atomic concentrations of C, O, N, Si, and Ti calculated from XPS intensities on surfaces **Ti**, **A**, **MH**, and **GMH**.

Maleimide-Modified Surface. The C 1s spectra of surface **MH** can be deconvoluted into four peaks with those at binding energies 289.0 and 288.2 eV being assigned to the newly introduced imide and amide functionalities, respectively. The N 1s emission has a new predominant contribution between 400 and 401 eV, again indicative of amide and imide functional groups reported to have binding energies of 400.1 and 400.7 eV, respectively.[31] The disappearance of the Ti $2p_{3/2}$ (metal) peak at 453.3 eV demonstrates that the total thickness of the oxide plus organic surface layer now exceeds the information depth of XPS (ca. 8 nm).

(29) Sittig, C.; Wieland, M.; Vallotton, P.-H.; Textor, M.; Spencer, N. D. *J. Mater. Sci. Mater. Med.*, in press.

(30) Kallury, K. M. R.; Macdonald, P. M.; Thompson, M. *Langmuir* **1994**, *10*, 492.

(31) Beamson, G.; Briggs, D. *High-Resolution XPS of Organic Polymers*; John Wiley & Sons Ltd.: New York, 1992.

Table 3. Surface Concentrations and Surface Coverages of Amino Group on Surface A, of Maleimidyl Group on Surfaces MH, MP, and MC, of RGD Group on Surfaces RMH, RMP, RMC, GMH, GMP, and GMC

surface	radiolabeling reagents	radioactivity (nCi/cm^2 ± s.d.)	surface concentration[a] (nmol/cm^2 ± s.d.)	surface coverage[a] (group/nm^2 ± s.d.)	calculated surface coverage[b] (group/nm^2)
A	[^{14}C]-FA	53.3 ± 5.4	1.0 ± 0.2	6.0 ± 1.2	
MH	[^{35}S]-Cys	8.2 ± 1.0	0.05−0.77	0.4−4.6	2.2 ± 0.5
MP	[^{35}S]-Cys	6.3 ± 0.8	0.04−0.71	0.2−4.3	1.7 ± 0.5
MC	[^{35}S]-Cys	5.6 ± 0.7	0.03−0.72	0.2−4.3	1.4 ± 0.4
RMH	[^{14}C]-PG	2.81 ± 0.43	0.052 ± 0.008	0.31 ± 0.05	0.3 ± 0.1
RMP	[^{14}C]-PG	2.17 ± 0.37	0.040 ± 0.007	0.24 ± 0.04	0.3 ± 0.1
RMC	[^{14}C]-PG	1.84 ± 0.27	0.034 ± 0.005	0.20 ± 0.03	0.2 ± 0.1
GMH	[^{14}C]-PG	3.27 ± 0.48	0.061 ± 0.009	0.37 ± 0.05	0.4 ± 0.1
GMP	[^{14}C]-PG	2.45 ± 0.40	0.045 ± 0.007	0.27 ± 0.04	0.3 ± 0.1
GMC	[^{14}C]-PG	2.33 ± 0.32	0.043 ± 0.006	0.26 ± 0.04	0.3 ± 0.1

[a] To calculate the surface concentration and surface coverage from the radioactivity, we assume the following molar ratios: [FA]/[NH_2] = 1, [Cys]/[Maleimidyl group] = $R_{X\rightarrow Y}$ in Table 2, respectively, [PG]/[RGD] = 2 (see text in section 3.4). The specific radioactivity of [^{14}C]-FA is 54.0 nCi/nmol, of [^{35}S]-Cys is between 20 and 150 *n*Ci/nmol, and of [^{14}C]-PG is 27.0 nCi/nmol. [b] The values are calculated by a combination of the NH_2 surface coverage on **A** and the reaction yields from Table 2. The errors correspond to calculated values.

MP and **MC** show similar XPS chemical shifts and the spectra are not shown here. The C 1s intensities above 288.0 eV are somewhat lower compared to those of **MH** and exhibit shoulders rather than obvious peaks (not shown here). This implies that the largest surface coverage occurs in the case of **MH**, which is consistent with results discussed below.

Peptide-Modified Surface. On the peptide-modified surface, **GMH**, no significant chemical shifts from **MH** were observed. The concentration of the newly introduced thiolether group is too low to be detected with confidence. The guanidinyl C 1s (289.0 eV) and amide C 1s (288.2 eV) overlap the imide and amide C 1s. Carboxyl, hydroxyl, and amide O 1s peaks at around 532 eV overlap Si−O and carbonyl O 1s. The guanidinyl (C=NH) N 1s at around 402 eV overlaps the protonated amines. However, the significant increase of the relative peak areas of N 1s, of O 1s above 532.0 eV, and of C 1s above 288.0 eV, as well as the decrease of the Ti 2p and Si 2p, are consistent with the presence of peptides.

3.3. Estimation of Reaction Yields. Atomic concentrations calculated from XPS intensities depend on the measured volume and the chemical components within this volume. Quantitative statements in regard to reaction yields for the subsequent modification reactions are difficult because of the inevitable carbon contamination and oxygen content on the starting surface **Ti**, and the changes of the chemical components and the film thickness on different surfaces. Although the average atomic concentrations reflect the sequential reactions well, the above-mentioned factors, as well as normal quantitative error, can result in a considerable deviation in the case of the low-concentration elements such as N and Si. Fortunately, silicon, which is not present on the starting surface, **Ti**, can be used as an internal reference. The absolute silicon surface content from **A** through **P** remains constant. Since the whole organic surface layer thickness is below the information depth of XPS, the atomic ratio of N to Si is a more representative parameter than the atomic concentration to follow quantitative surface changes. The reaction yields can be deduced from the following simple formula:

Reaction yield (**A** → **M**) = (imide-*N* content on **M**)/(*N* content on **A**)

$$R_{A\rightarrow M} = \frac{n_{N(M)} - n_{N(A)}}{n_{N(A)}} = \frac{(N/Si)_M - (N/Si)_A}{(N/Si)_A} \quad (1)$$

Reaction yield (**M** → **P**) = [(peptide-*N* content on **P**)/*m*]/(imide-*N* content on **M**)

$$R_{M\rightarrow P} = \frac{(n_{N(P)} - n_{N(M)})/m}{n_{N(M)} - n_{N(A)}} = \frac{[(N/Si)_P - (N/Si)_M]/m}{(N/Si)_M - (N/Si)_A} \quad (2)$$

where $R_{X\rightarrow Y}$ is the reaction yield from *X* to *Y*, $n_{N(i)}$ is the absolute nitrogen content of surface *i*, and $(N/Si)_i$ is the atomic ratio of N to Si on surface *i*. The divisor *m* takes account of the *m* nitrogen atom(s) in one peptide molecule (1 for cysteine, 7 for RGDC, and 10 for GRGDSPC).

The calculated reaction yields are summarized in Table 2. EMCS in the reaction **A** → **MH** shows the highest reaction yield among the three cross-linkers, suggesting the importance of steric hindrance. SMP has a short chain of three methylene groups between succinimidyl ester and maleimide, SMCC a bulky cyclohexane, while EMCS has a longer chain of six methylene groups. The former two have more rigid structures than the latter. One possible explanation is that EMCS, due to its molecular flexibility, has a higher probability of reaching partially occupied, reactive sites on the surface. Another factor could be the molecular organization on the surface: Because of the shorter spacer and molecular configuration, MP and MC groups are bound close to the binding sites, leading to increased disorder on a macroscale, and occupying more space. Particularly in the valley areas, the steric hindrance from the occupied maleimidyl group could largely inhibit the accessibility of the surface. However, for the MH group, the relatively longer spacer with its potential for greater interchain van der Waals interactions may result in some long-range ordering.

For thioether formation, the molecular size seems to be the key factor affecting the reaction yields. This might be the reason for the high yield (up to 80%) for cysteine and the generally low yields (about 18%) for RGDC and GRGDSPC.

3.4. Surface Coverage. Quantitative surface coverages were determined using radiolabeling techniques. [^{14}C]-Formaldehyde, [^{35}S]-cysteine, and [^{14}C]-phenylglyoxal were employed to measure the surface coverage of primary amine in **A**, maleimide in **M**, and peptide in **P**, respectively.

The surface coverages of maleimide and peptide were additionally estimated on the basis of the radiolabeling-derived amine surface concentration on **A** and the XPS-derived reaction yields shown in Table 2. These data are in quite good agreement with the directly measured values (see Table 3).

[^{14}C]-Formaldehyde Radiolabeling on Silanized Surfaces. [^{14}C]-Formaldehyde with $NaBH_3CN$ has been used as a standard procedure to label the free amino groups

of proteins.[32] The primary amine reacts first with formaldehyde to form a Schiff base, which is then reduced by $NaBH_3CN$ to the secondary amine. Although the secondary amine can again react and form the tertiary amine, the stoichiometry of $[NH_2]/[H_2CO]$ can be fairly well-controlled to 1 under appropriate reaction conditions. We carried out the reaction in CH_3CN solution at 20 °C for 4 h. It is assumed that the small formaldehyde molecule can diffuse into the open-structure APS film and react with all the primary amine groups. With this assumption, the surface concentration (1.0 nmol/cm^2) and coverage (6.0 group/nm^2) of primary amines can be simply calculated from the specific radioactivity and the radiolabeled area. To exclude contributions from physically adsorbed ^{14}C-labeled formaldehyde, the surfaces of **Ti** and acetylated **A** were used as controls. Only negligible amounts of about 1 nCi/cm^2 (0.02 nmol/cm^2) were detected in these cases.

[^{35}S]-Cysteine Radiolabeling on Maleimide-Modified Surfaces. [^{35}S]-Cysteine was chosen to label the maleimidyl groups because of two reasons: (1) To mimic the reaction of terminal cysteine on peptides with maleimidyl groups; (2) to evaluate the surface coverage and reactivity of maleimide since maleimidyl groups may hydrolyze to maleamic acid. A still open question is whether cysteine reacted completely with maleimide or not. The estimated reaction yields from XPS were used to calculate the maleimide coverage. The estimated surface coverages of maleimide are only semiquantitative, however, since the specific radioactivity is specified by the supplier as 20−150 mCi/mmol. Surface **A** and the unlabeled-cysteine-reacted surface **M** were used as the control surfaces. Only negligible amounts of around 1 nCi/cm^2 on control surfaces were detected and thus supported the covalent nature of the bond.

[^{14}C]-Phenylglyoxal Radiolabeling on Peptide-Modified Surfaces. A standard target reaction of the guanidinyl moiety of arginine residues is with 1,2-dicarbonyl reagents.[33] Under mild alkaline conditions, these compounds condense with the guanidinyl group in an initial reaction very similar to the Schiff base formation, which is followed by further rearrangement to form different products. Arginine-containing peptides or proteins can form adducts with phenylglyoxal in a stoichiometric ratio (phenyglyoxal/arginine) of 1 or 2 depending on the peptides or proteins involved, and the reaction conditions. Following a published procedure,[34] we carried out the reaction in 25 mM sodium phosphate buffer (pH 7.4) at 20 °C for 24 h. A stoichiometry of 2 phenylglyoxal to 1 arginine is assumed here to calculate the peptide surface coverages. Both the direct radiolabeling measurements and the indirect calculation from the estimated reaction yields indicate surface coverages in the same range of 0.2−0.4 molecules/nm^2. According to a molecular modeling study, the minimum energy conformation of GRGDSPC (Figure 1) has dimensions of about 2 × 1 nm^2. Assuming equidistant attachment sites, this would correspond to an average separation of 2.2 nm of GRGDSPC on surface **GMH**.

3.5. Optimization of Conjugation Reactions. Surface A to Surface M. The linkers serve two purposes: (1) To covalently bind two distinct chemical entities that otherwise would remain unreactive toward each other; (2) to provide a physical spacer allowing for greater accessibility and/or orientational freedom of the attached biomolecules.

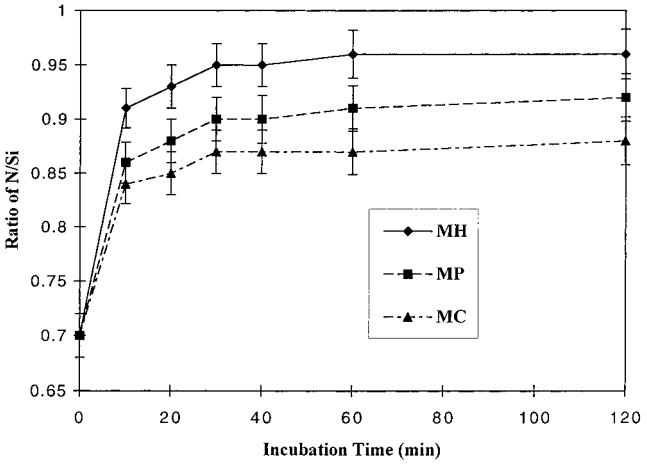

Figure 5. The relationship between the atomic ratios N/Si (XPS) on the maleimide-modified surfaces and the incubation time.

The succinimidyl ester reacts preferentially with amino groups, eliminating *N*-hydrosuccinimide as the leaving group. The reaction in solution is complete within 10−20 min at pH 6−9.[35] The competing reaction is the hydrolysis of the succinimidyl ester. The reaction was carried out in different solvents (e.g., aqueous buffer, *N*,*N*-dimethyl formamide (DMF), dimethyl sulfoxide (DMSO), and acetonitrile). The highest yield was achieved in CH_3CN, while an aqueous buffer is least suitable due to the low solubility of the cross-linkers and the hydrolysis of both the succinimidyl ester and the maleimide.

The effect of cross-linker concentration in the range of 1.0−10.0 mM was checked by XPS; no obvious differences were observed with a molar ratio of 2 cross-linkers to 1 primary amine. Thus, a 5.0 mM solution was used as the standard. All the experiments were carried out at 20 °C under an ambient atmosphere. The main variable is the reaction time, which is an important parameter, controlling both the extent of reaction and the surface uniformity. Figure 5 shows the relationship of the atomic ratio N/Si (XPS) with the incubation time. The reaction is very fast within the first 10 min, reaching its maximum after approximately 30 min.

Surface M to Surface P. Maleimides are quite specific to the thiol group, especially at pH < 7 where other nucleophiles are protonated. In acidic and near-neutral solutions, the reaction rate with simple thiols is about 1000-fold faster than with the corresponding simple amines.[36] The other major competing reaction is the hydrolysis of maleimide to maleamic acid. However, this reaction is much slower than the thiolether formation in near-neutral solutions. At pH 7, it is estimated that the half-life reaction time between millimolar concentrations of mercaptan and maleimide is of the order of 1 s.[36] The resulting thioether bond is very stable and cannot be cleaved under physiological conditions. The peptide modification was carried out in an aqueous solution. Samples treated in different concentrations and incubation times were evaluated by XPS. The effect of varying the peptide concentration in the range of 0.1−5 mM was not significant. Figure 6 shows the effect of incubation time on the atomic ratio N/Si (XPS). A sharp increase in the peptide surface concentration takes place in the first 20

(32) Jentoft, N.; Dearborn, D. G. *J. Biol. Chem.* **1979**, *254*, 4359.
(33) Yankeelov, J. A., Jr. *Methods Enzymol.* **1972**, *25*, 566.
(34) Liao, T.-H.; Ho, H.-C.; Abe, A. *Biochim. Biophys. Acta* **1991**, *1079*, 335.
(35) Lindsay, D. G. *FEBS Lett.* **1972**, *21*, 105.
(36) Glaser, A. N. In *The Proteins*, 3rd ed.; Neurath, H., Hill, R. L., Eds.; Academic Press: New York, 1976; Chapter 2.

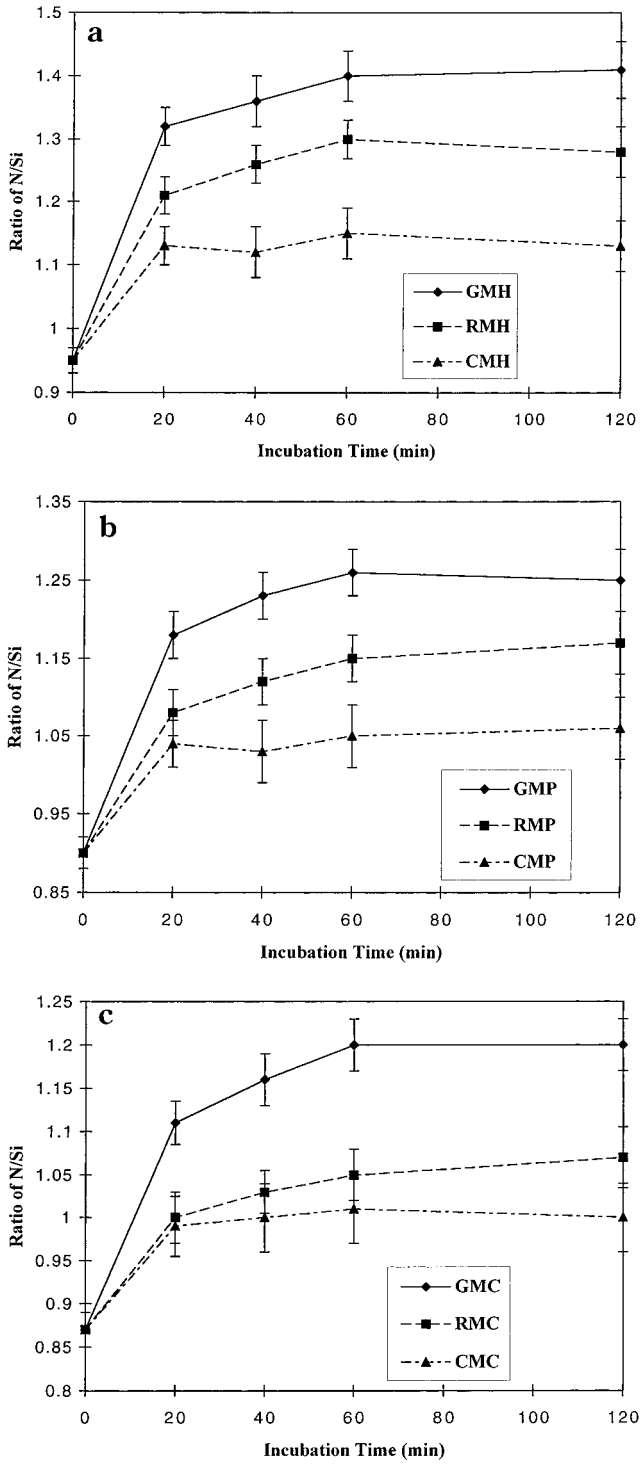

Figure 6. The dependence of the atomic ratios N/Si (XPS) of the peptide- or L-cysteine-modified surfaces on the incubation time.

min, followed by a slow increase. A reaction time of 1 h was chosen for the standard protocol. Although N/Si slowly increases with longer incubation times, this could be due to hydrolysis of siloxane films.

Degradation in Water. A problem related to the application of immobilized biomolecules via silanization techniques is the bioactivity loss due to hydrolysis of the siloxane films. Degradation was followed by measuring the radioactivity loss of the radiolabeled samples immersed in water (Figure 7). Comparing degradation kinetics of the different surfaces, **^{14}CA**, **^{35}SMH**, and **^{14}CGMH**, the main origin for the loss of peptide functionality appears

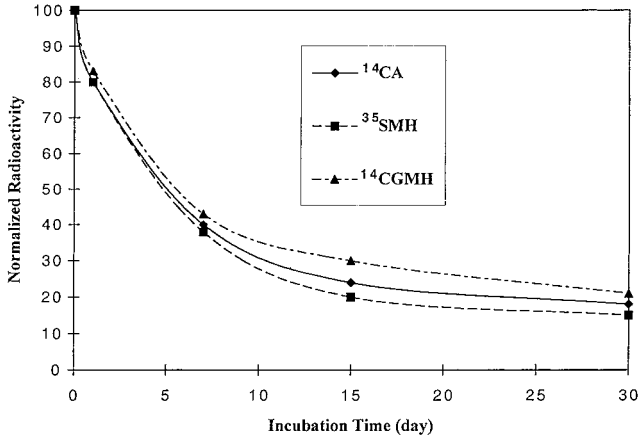

Figure 7. The degradation of **^{14}CA**, **^{35}SMH**, and **^{14}CGMH** in water measured through the loss of radioactivity. The data are normalized to the initial value.

to be the hydrolysis of siloxane films. A loss of about 50% occurs in the first week, followed by a gradual loss over several months.

3.6. Infrared Reflection Absorption Spectroscopy Measurements. Infrared reflection absorption spectroscopy (IRAS) has been thoroughly described.[37] It relies on reflecting an infrared beam at near-grazing incidence from the mirrorlike metallic surface on which the thin film of interest has been deposited. Since the surface roughness of the modified samples is much smaller ($R_a \approx$ 1.7 nm from AFM data) than the wavelength of the IR radiation, the electric field vector of the incident and reflected beams in our IRAS studies is expected to be along the normal of the surface plane. Hence, only the surface normal component of the dipole moment change can interact with the IR standing wave electric field at the surface, since the field vector and dipole moment derivative vector must be parallel. Thus, information on the orientation of the IRAS-active functional groups can be obtained.

Different infrared techniques have been applied to study the APS structure on silica[38] and metal surfaces.[27] Generally, the broad strong bands occur around 1140 cm^{-1} and are due to the Si−O−Si antisymmetric stretching mode. Absorption bands around 1570 cm^{-1} are caused by amine groups, but these were not detected in our case because of the low thickness of APS films (Figure 8).

The cyclic imide carbonyl groups in the crystalline state or in liquid solution exhibit at least two bands in the 1700−1800-cm^{-1} region.[39] One band is located between 1800 and 1740 cm^{-1} (symmetric stretch) and a more intense band between 1740 and 1700 cm^{-1} (antisymmetric stretch). The separation of the two bands is due to vibrational coupling of the carbonyls, leading to symmetric and antisymmetric stretching modes (Figure 9). Various explanations have been offered[39] for the symmetric and antisymmetric carbonyl stretch being assigned at the higher and lower frequency, respectively. These explanations include mechanical coupling, hydrogen bonding, and electronic effects. The antisymmetric vibration of the O=C−N−C=O group alternatively stabilizes the two resonance structures with a positive coupling constant lowering the frequency of the antisymmetric vibration.

(37) Allara, D. L.; Nuzzo, R. G. *Langmuir* **1985**, *1*, 52.
(38) Vandenberg, E. T.; Bertilsson, L.; Liedberg, B.; Uvdal, K.; Erlandsson, R.; Elwing, H.; Lundström, I. *J. Colloid Interface Sci.* **1991**, *147*, 103.
(39) (a) Mckittrick, P. T.; Katon, J. E. *Appl. Spectrosc.* **1990**, *44*, 812. (b) Parker, S. F. *Spectrochim. Acta, Part A* **1995**, *51*, 2067. (c) Matsuo, T. *Bull. Chem. Soc. Jpn.* **1964**, *37*, 1844.

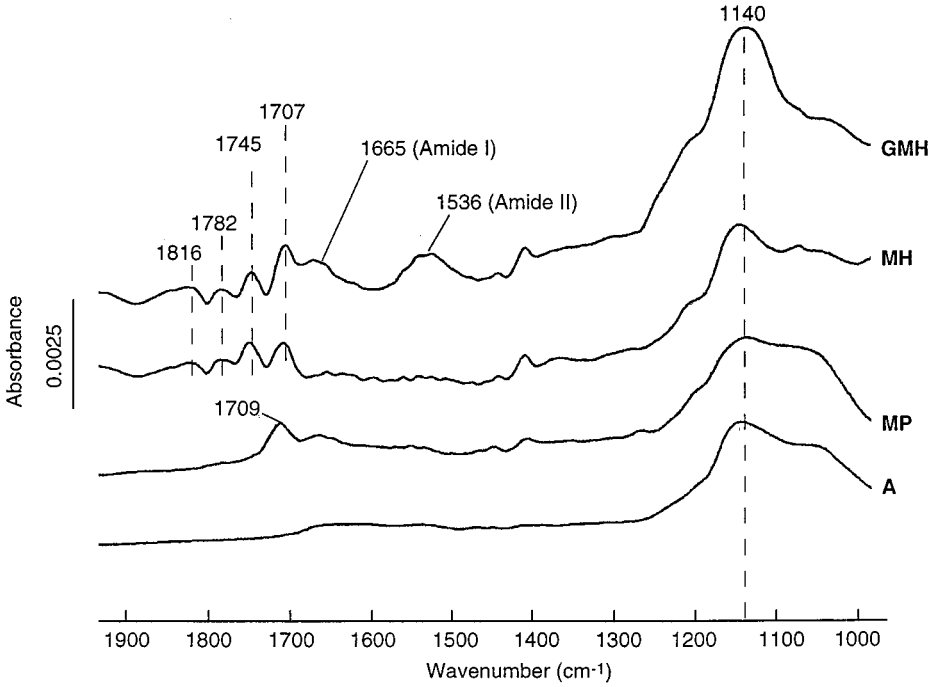

Figure 8. Infrared reflection spectra (IRAS) of surfaces **A**, **MP**, **MH**, and **GMH**.

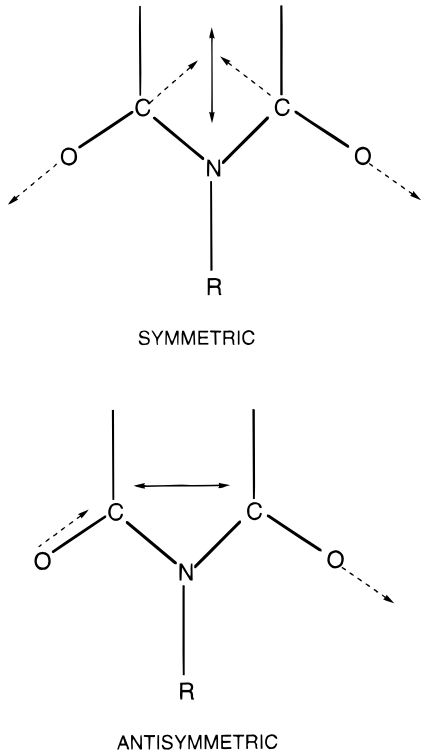

Figure 9. Symmetric and antisymmetric stretching vibrations of the imide moiety. Both-end-arrow lines represent the directions of the transition dipole moments.

On the **MP** and **MC** surfaces, only the antisymmetric vibration at 1709 cm^{-1} is clearly observed, while the symmetric one above 1740 cm^{-1} is barely detected, similar to the intensity distribution of polycrystalline maleimide derivatives with random orientation. However, on the **MH** surface, in addition to the antisymmetric vibration of the maleimidyl group at 1707 cm^{-1}, there are three other peaks at 1745 (strong), 1782 (weak), and 1816 (weak) cm^{-1}. The reason for these differences is not yet clearly understood and is under further investigation. A possible explanation is the presence of byproducts of an unknown side reaction. Another, more likely, explanation is a statistically preferential orientation of the molecules on surface **MH**. In this case, we tentatively assign 1745 cm^{-1} to the symmetric stretching mode of maleimide. The stronger intensity of this peak compared to those of the polycrystalline maleimide derivatives with random orientation may be attributed to a preferred orientation or aggregation of the maleimidyl groups, since the surface selection rule requires that the transition dipole moment of the symmetric stretching mode (Figure 9) has a substantial component along the substrate surface normal.

After the peptide attachment step, part of the maleimide is converted to succinimide. The bands of cyclic imide carbonyl groups appear virtually unchanged (Figure 8, **GMH**). The main difference between maleimide and succinimide is the fact that succinimide has a much stronger band around 1200 cm^{-1} (C−N−C).[39] The increased absorption intensity around 1200 cm^{-1} is attributed to the stretching vibration of C−N−C of succinimide and/or amide III (ca. 1200 cm^{-1}). Another obvious character on **GMH** is the enhanced amide groups. Additional information can be gained in the amide vibration regions: amide I at around 1660 cm^{-1} and amide II at around 1540 cm^{-1} are the characteristic absorption bands for peptides and proteins. Although an amide group is already present on **MH** before coupling the peptides, the strong increase in intensity at 1665 cm^{-1} (amide I) and at 1536 cm^{-1} (amide II) on surface **GMH** reflects the increased number of amide functionalities.

Conclusions

In summary, a three-step reaction procedure was employed to attach RGD-containing peptides onto a titanium surface. First, water−vapor−plasma-pretreated titanium surfaces were silanized with (3-aminopropyl)-triethoxysilane in dry toluene, resulting in a multilayer film of poly(3-aminopropyl)siloxane. Second, the free primary amino groups were linked to one of the three hetero-cross-linkers: *N*-succinimidyl-6-maleimidylhexanoate, *N*-succinimidyl-3-maleimidylpropionate, and *N*-

succinimidyl *trans*-4-(maleimidylmethyl)cyclohexane-1-carboxylate. Finally, onto the resulting terminal-maleimide surface, two model, cell-adhesive peptides, H-Gly-Arg-Gly-Asp-Ser-Pro-Cys-OH (GRGDSPC) and H-Arg-Gly-Asp-Cys-OH (RGDC), were immobilized through covalent addition of the cysteine thiol (−SH) group. X-ray photoelectron spectroscopy (XPS), infrared reflection absorption spectroscopy (IRAS), and radiolabeling techniques were applied to characterize the surfaces. The main results are as follows: (1) Silanization on Ti surfaces is shown to be the key step in terms of reproducibility in the subsequent modification steps. Samples produced in one batch with a surface coverage of 6 amino groups/nm^2 were used for further surface reactions. (2) The maleimidyl group introduced in the second-step reaction has been characterized using XPS (binding energy of C 1s at 289.0 eV), IRAS (band at around 1707 cm^{-1}), and radiolabeling techniques with [^{35}S]-cysteine. (3) The atomic ratio N/Si determined by XPS is used to estimate the reaction yields and to follow the reaction kinetics. The reaction yields are estimated to be about 30% for the reaction step of the aminosiloxane to the maleimide surface and about 18% for the conversion of the maleimide to the peptide surface. Optimal incubation times are 30 min for the former reaction and 1 h for the latter. (4) The grafted peptides, RGDC and GRGDSPC, have been qualitatively and quantitatively characterized with XPS, IRAS, and [^{14}C]-phenylglyoxal radiolabeling techniques. The surface coverage is estimated to be 0.2−0.4 peptide molecules/nm^2.

Acknowledgment. The authors would like to thank Dr. P. Böni and Mr. M. Horisberger of the Paul Scherrer Institute (PSI), CH-5232 Villigen PSI, for Ti coating, Mr. S. Brunner of the Department of Materials at ETH Zurich for technical help in IRAS measurements, Dr. M. Morstein of the Laboratory for Surface Science and Technology for generating the space-filling model of GRGDSPC, Dr. H. Chai-Gao and Ms. O. Bucher of CSEM for technical help at the beginning of this work, Dr P.-H. Vallotton of Institut Straumann, CH-4437 Waldenburg, and Mr. M. Windler of Sulzer Orthopedics, CH-8404 Winterthur, for their support. We are grateful to the Swiss Priority Program on Materials (PPM) (Council of the Swiss Federal Institutes of Technology) for their generous financial assistance.

LA980257Z